Editors' Suggestion

MicroBooNE and the ν_e Interpretation of the MiniBooNE Low-Energy Excess

C. A. Argüelles,[1] I. Esteban,[2,3] M. Hostert,[4,5,6] K. J. Kelly,[7] J. Kopp,[7,8] P. A. N. Machado,[9] I. Martinez-Soler,[1] and Y. F. Perez-Gonzalez[10]

[1]*Department of Physics & Laboratory for Particle Physics and Cosmology, Harvard University, Cambridge, Massachusetts 02138, USA*
[2]*Center for Cosmology and AstroParticle Physics (CCAPP), Ohio State University, Columbus, Ohio 43210, USA*
[3]*Department of Physics, Ohio State University, Columbus, Ohio 43210, USA*
[4]*Perimeter Institute for Theoretical Physics, Waterloo, Ontario N2J 2W9, Canada*
[5]*School of Physics and Astronomy, University of Minnesota, Minneapolis, Minnesota 55455, USA*
[6]*William I. Fine Theoretical Physics Institute, School of Physics and Astronomy, University of Minnesota, Minneapolis, Minnesota 55455, USA*
[7]*Theoretical Physics Department, CERN, Esplande des Particules, 1211 Geneva 23, Switzerland*
[8]*PRISMA+ Cluster of Excellence & Mainz Institute for Theoretical Physics, Staudingerweg 7, 55128 Mainz, Germany*
[9]*Particle Theory Department, Fermi National Accelerator Laboratory, Batavia, Illinois 60510, USA*
[10]*Institute for Particle Physics Phenomenology, Durham University, South Road, Durham DH1 3LE, United Kingdom*

(Received 6 December 2021; revised 14 March 2022; accepted 20 April 2022; published 13 June 2022)

A new generation of neutrino experiments is testing the 4.7σ anomalous excess of electronlike events observed in MiniBooNE. This is of huge importance for particle physics, astrophysics, and cosmology, not only because of the potential discovery of physics beyond the standard model, but also because the lessons we will learn about neutrino-nucleus interactions will be crucial for the worldwide neutrino program. MicroBooNE has recently released results that appear to disfavor several explanations of the MiniBooNE anomaly. Here, we show quantitatively that MicroBooNE results, while a promising start, unquestionably do not probe the full parameter space of sterile neutrino models hinted at by MiniBooNE and other data, nor do they probe the ν_e interpretation of the MiniBooNE excess in a model-independent way.

DOI: 10.1103/PhysRevLett.128.241802

Introduction.—Sterile neutrinos have been postulated to explain various anomalies in neutrino experiments [1], in particular the excess of electron-neutrino events in the LSND [2] and MiniBooNE [3] experiments. If real, sterile neutrinos would revolutionize our understanding of early-Universe cosmology [4], modify neutrino emission from astrophysical sources [5–7], and force a reevaluation of the standard model of particle physics. Precision measurements in cosmology, astrophysics, and particle physics will remain ambiguous until we clarify whether such sterile neutrinos exist.

Recently, the MicroBooNE Collaboration has released results scrutinizing the MiniBooNE low-energy excess (MBLEE). As the MicroBooNE detector is exposed to the same neutrino beam as MiniBooNE but has superior event reconstruction capabilities, it is able to differentiate between different interpretations of the MBLEE. A first MicroBooNE analysis disfavors that the MBLEE is due to underestimated production of Δ baryons followed by decays to photons at a significance of 94.8% C.L. [8].

Three distinct, complementary analyses have since been released, addressing whether the MBLEE is caused by an excess of electron-neutrinos in the beam [9–12]. These analyses compare the MicroBooNE data to a signal template defined by the assumption that the expected spectrum of the ν_e excess in MiniBooNE exactly matches the difference between the data and the best-fit background prediction. Assuming this nominal template, the collaboration concludes that "the results are found to be consistent with the nominal ν_e rate expectations from the Booster Neutrino Beam and no excess of ν_e events is observed" [9].

However, as we show below, this approach is insufficient to exclude the ν_e interpretation of the MBLEE in a model-independent way, or even to exclude the sterile neutrino solution of the MBLEE. It is important to explicitly address these questions, as they directly impact the future of the short-baseline neutrino program as well as a variety of alternative models [13–18] proposed to explain the MiniBooNE and LSND results. Previous attempts to constrain the LSND and MiniBooNE excesses suffered from insufficient sensitivity to cover the allowed parameter space [19–23], so the power of MicroBooNE must be quantified as we search for definitive answers to this 20-year-old

puzzle. That is the goal of this Letter. We first analyze the constraints of MicroBooNE's latest results on ν_e appearance in MiniBooNE in a model-independent way, then we narrow our focus to sterile neutrinos. While doing this, we provide a methodology to analyze data that we hope will help in making future claims more robust. We make all analysis tools and results fully public in Ref. [24].

For the first stage, we follow the MicroBooNE procedure: starting from a MiniBooNE event spectrum, we derive an expected excess of events in MicroBooNE, and we perform a statistical analysis of the data. After verifying that we reproduce MicroBooNE's results when using their nominal template, we repeat the analysis with a set of alternative templates that are equally successful at explaining the MBLEE. These alternative templates are allowed due to the relatively large, nontrivial uncertainties in MiniBooNE.

For the second stage, we perform a fit of MicroBooNE data to a simple light sterile neutrino model. We assume both a simplified oscillation scenario with only $\nu_\mu \to \nu_e$ appearance, as well as a fully consistent oscillation model that accounts for oscillations in the MicroBooNE control samples and backgrounds.

Experimental analysis.—To quantify the disagreement between MicroBooNE data and a ν_e interpretation of the MBLEE, we proceed as follows. All our analyses start with a hypothesis for the MBLEE [25]. To obtain the expected spectrum at MicroBooNE, we rescale the spectrum to account for the differences in exposure and detector mass between MiniBooNE and MicroBooNE [9]. We then smear the events according to MicroBooNE's energy resolution [10,11]. Finally, to infer MicroBooNE's energy-dependent ν_e detection efficiency, we apply all previous steps to the intrinsic ν_e background, and we choose the efficiency in each reconstructed energy bin such that our results match the official MicroBooNE background prediction [10,11]. We have checked that our efficiencies are consistent with the energy-averaged efficiencies quoted in Refs. [10,11], and that they generate an MBLEE prediction that matches the official MicroBooNE result. Our Supplemental Material [27] provides more detail about checks and comparisons with the MicroBooNE expectations.

We focus on the charged-current inclusive [10] and quasielastic (CCQE) [11] channels, [28] as they comprise the leading statistical power of MicroBooNE, and we use the provided data releases wherever possible [29,30]. For the inclusive analysis, we have performed several statistical tests, including both Pearson-χ^2 and CNP-χ^2 [31], as well as calculating a test statistic with or without deriving a constraint using the conditional covariance matrix formalism [10]. For all tests, we find very good agreement with the results of Ref. [10]. For clarity, in what follows we perform all statistical tests using the CNP-χ^2 formalism with the full (137,137) covariance matrix of Refs. [10,29]. For the CCQE analysis, in turn, we use a Poisson likelihood, where the expectation in each bin is treated as a nuisance parameter that is constrained by the covariance matrix. Our test statistic in this latter analysis is then determined by profiling over these nuisance parameters.

Template results.—Our first approach assesses whether MicroBooNE generically rules out a ν_e interpretation of the MBLEE. In particular, the MiniBooNE signal has large, nontrivial, multiply signed uncertainties. These allow for different shapes of the MBLEE that could affect the prediction at MicroBooNE.

We generate a set of MBLEE templates using a Markov-Chain Monte Carlo (MCMC) [32] by independently rescaling the normalization of the MiniBooNE backgrounds. Our template for the MBLEE is then given by the difference between the observed data and the rescaled backgrounds [33]. We group backgrounds in four classes: intrinsic ν_e, misidentified π^0, $\Delta \to \gamma$, and all others. To estimate how well each template fits the MiniBooNE data, we calculate its goodness-of-fit p-value using a χ^2 test statistic with the MiniBooNE covariance matrix [34]. We follow the MiniBooNE prescription, that the test-statistic follows a χ^2 distribution with 8.7 degrees of freedom (while our template model has 4 d.o.f.).

This generates a set of MBLEE templates compatible with MiniBooNE. To translate them to MicroBooNE, we have to generate an MBLEE template *before* MiniBooNE detector effects. For this, we apply the D'Agostini iterative unfolding method [35,36], making use of the MiniBooNE response matrix [37,38]. We have checked the accuracy of our procedure for a variety of spectra (see Supplemental Material [27]). We do not assign any uncertainty to this procedure, as the purpose of unfolding is just to inspire some choices of MBLEE spectra and see if some are compatible with MiniBooNE and MicroBooNE.

Figure 1 demonstrates our procedure. We show three different MiniBooNE templates (upper panel) and the corresponding predicted MicroBooNE excesses (lower panel): the nominal template given by the difference between the observed data and the best-fit background estimate (solid black); a template with significantly more events at low energies but a p-value of 87% (blue); a template with fewer events and a p-value of 87% (red); and a template given by the best-fit $\nu_\mu \to \nu_e$ two-neutrino oscillations, corresponding to $\Delta m^2 = 0.041$ eV^2 and $\sin^2 2\theta = 0.92$, which has a p-value of 20% (dotted black).

As we see, MiniBooNE uncertainties allow for very different shapes and rates of the MBLEE (including those coming from the sterile neutrino hypothesis) to provide a good fit to the data. These generate different predictions at MicroBooNE that will be excluded with a different statistical significance. This is crucial in constraining the interpretation of the MBLEE in terms of ν_e events at MicroBooNE.

For the template analysis results, we focus on the inclusive channel, which provides the best constraints on

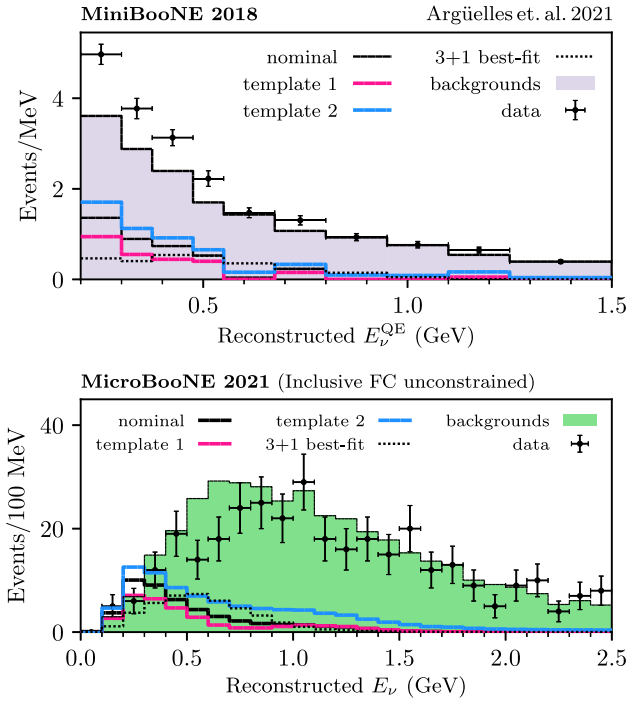

FIG. 1. Event rate at MiniBooNE (top) and MicroBooNE (bottom) as a function of reconstructed neutrino energy. We show several MiniBooNE templates, including that of the $3+1$ oscillation best-fit, as nonstacked histograms. The bottom panel shows the spectra predicted by these templates in the MicroBooNE Inclusive fully contained channel.

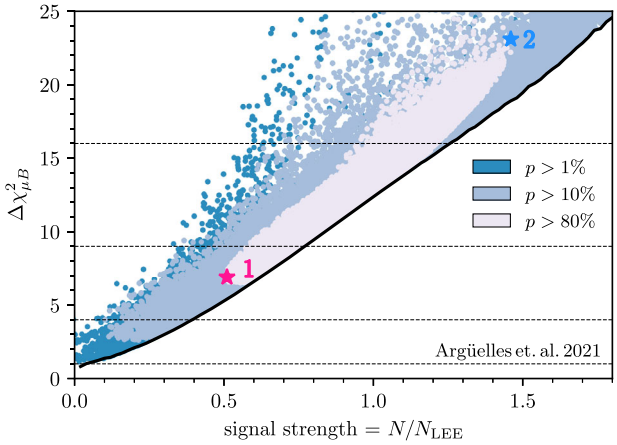

FIG. 2. $\Delta\chi^2$ of the MicroBooNE Inclusive analysis with respect to the no-excess hypothesis, for various templates found by our MCMC. Each point corresponds to a specific template that provides a good fit to MiniBooNE data with a p-value greater than 80%, 10%, and 1% (shades of blue). The stars correspond to templates 1 and 2 presented in Fig. 1.

the ν_e interpretation of the MBLEE. We organize the templates in three categories by decreasing goodness of fit, $p > 80\%$, 10%, and 1%; and classify them by their signal strength, defined as $N/N_{\rm LEE}$ with N the number of excess events that the template predicts at MiniBooNE and $N_{\rm LEE} = 360$ the observed number of excess events.

Figure 2 shows the result of the template analysis. Each point corresponds to a different template, colored according to the three goodness-of-fit categories defined above. For each template, we compute the corresponding MicroBooNE $\chi^2_{\mu B}$, and construct the difference with respect to the no-excess hypothesis, $\Delta\chi^2_{\mu B}$. We also show as a black line the result of profiling over all templates with the same signal strength. The horizontal lines then correspond to the MicroBooNE 1, 2, 3, and 4σ exclusion limits [39,40].

As we see in Fig. 2, introducing shape and normalization uncertainties in the MBLEE template can either enhance or mitigate MicroBooNE's sensitivity. To illustrate the variability of the template shapes and normalizations, we have marked with a star the two templates shown in Fig. 1, corresponding to two extreme points in the $p > 80\%$ region.

Many templates that are a good fit to MiniBooNE data cannot be excluded by MicroBooNE—we observe a large number of templates with good fits to MiniBooNE data, $p > 80\%$ (10%), well below the $\Delta\chi^2_{\mu\rm B} = 9$ (4) line. We thus conclude that, while recent MicroBooNE results indeed constrain the ν_e interpretation of the MiniBooNE excess in a model-independent way, they do not completely rule it out. Because of the correlated systematic uncertainties between MiniBooNE and MicroBooNE, to fully establish the compatibility of these templates, a joint analysis is required.

Sterile Neutrino analysis.—The analysis above does not rely on any specific particle physics model. As an example of a physics model that can explain the MBLEE, we turn to light sterile neutrinos. They provide a simple scenario that could lead to $\nu_\mu \to \nu_e$ transitions at short baselines, and have been extensively studied in the literature [1,4,41–43]. Here, we do not rely on the unfolding technique discussed above, as we simulate expected distributions in MiniBooNE with respect to the true neutrino energy.

To perform analyses including sterile neutrinos, we use Ref. [44] and first calculate, as a function of oscillation parameters, the expected MBLEE. Using the same procedure discussed above, we map these spectra into the expected excesses in MicroBooNE's inclusive and CCQE analyses. Leveraging [29,30], we can also account for oscillations of the ν_μ and ν_e charged-current (CC) background expectations in MicroBooNE's analyses to allow for a complete, four-neutrino oscillation analysis [45].

We start by discussing the results of the simplified sterile neutrino model, which assumes the backgrounds to be independent of the sterile neutrino parameters. This simplified model is parametrized by a squared-mass difference Δm^2_{41} and an effective mixing angle $\sin^2 2\theta_{\mu e} \equiv 4|U_{e4}U_{\mu 4}|^2$ with U the leptonic mixing matrix.

Figure 3 presents the results of our analyses of MicroBooNE's Inclusive and CCQE channels in blue and orange, respectively, at 3σ C.L. We first note that the Inclusive analysis has more constraining power than the

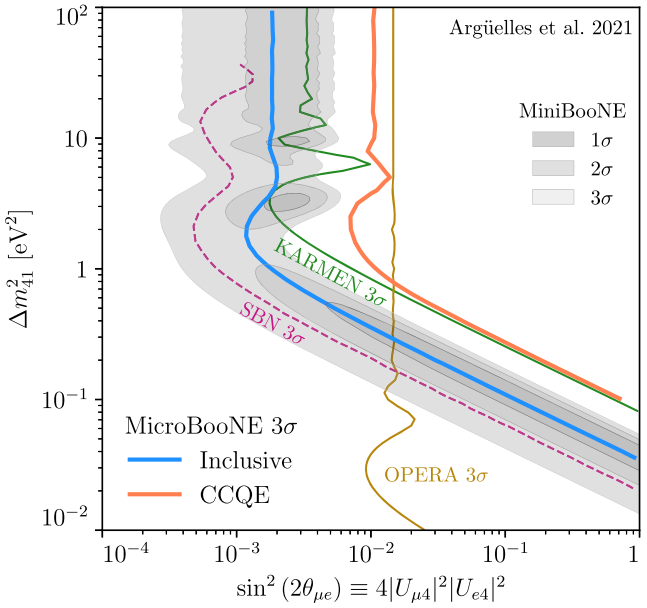

FIG. 3. MicroBooNE constraints on sterile neutrino parameter space at 3σ C.L. (blue, inclusive and orange, CCQE). For reference, we show the MiniBooNE 1-, 2-, and 3-σ preferred regions in shades of gray [26], the future sensitivity of the three SBN detectors (pink) [46], and existing constraints from KARMEN (green) [19] and OPERA (gold) [47].

CCQE analysis. This can be traced back to the detection efficiencies, which for the MiniBooNE and MicroBooNE CCQE analyses decrease at large energies, while in the Inclusive MicroBooNE analysis they stay constant. As sterile neutrinos predict a non-negligible excess at high energies, the inclusive analysis is more powerful.

As we see from Fig. 3, MicroBooNE data, at 3σ C.L., disfavor part of the region preferred by MiniBooNE at the same C.L. Nevertheless, we find that there is still a large viable fraction of the parameter space, even within 1σ C.L. preferred region of MiniBooNE. We find it unlikely that future MicroBooNE results will significantly improve on this, even though MicroBooNE has only analyzed about half of their dataset, because of a deficit in their inclusive data that generates more sensitivity than expected (cf. Fig. 1 and the Supplemental Material [27]; this could be due to an underfluctuation in the data or to background mismodeling). This highlights the importance of searching for sterile neutrinos with the three SBN detectors—SBND, MicroBooNE, and ICARUS—which will probe the full 2σ region preferred by MiniBooNE with less dependence on the neutrino cross section and flux.

Finally, we stress that a fully consistent four-neutrino analysis should also consider oscillations of the backgrounds. This is relevant at MiniBooNE [16,48], and even more for the MicroBooNE inclusive analysis: while the former has large non-neutrino induced backgrounds, the dominant background in the latter is beam-ν_e contamination. Moreover, since other neutrino samples (particularly,

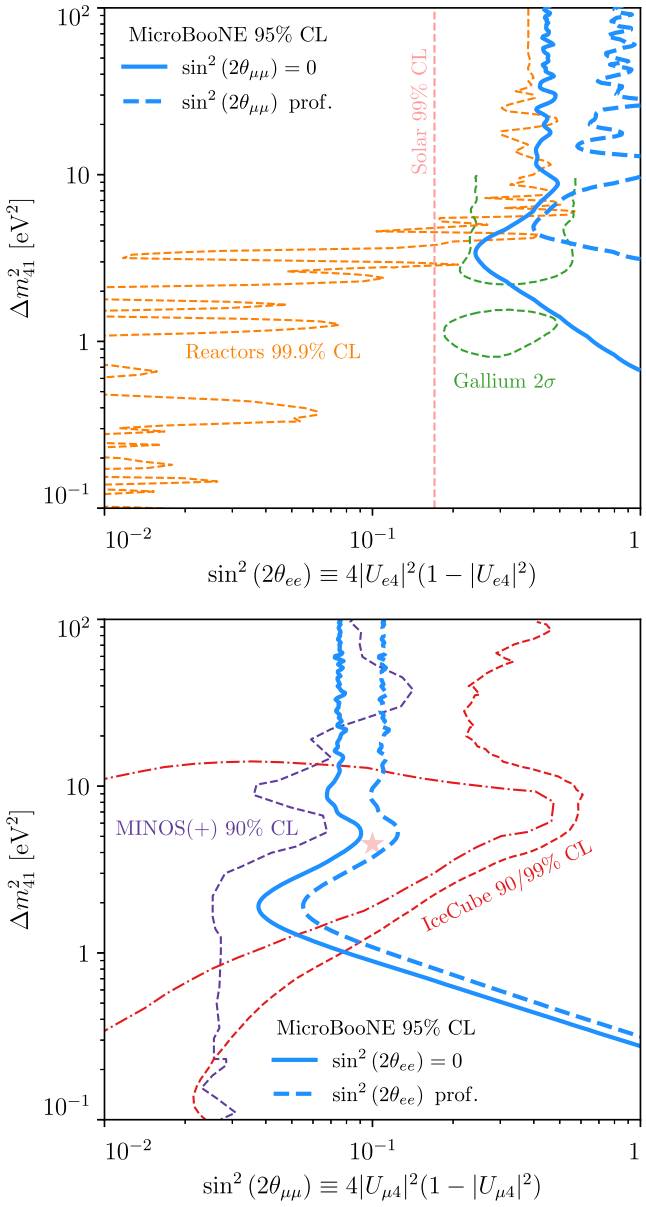

FIG. 4. MicroBooNE constraints on Δm^2_{41} and $\sin^2(2\theta_{ee})$ (left) or $\sin^2(2\theta_{\mu\mu})$ (right). In each panel, we have either fixed (solid lines) or profiled over (dashed) the unshown mixing angle. For comparison, we show existing constraints and preferred regions (see Refs. [49–63]).

CC ν_μ) are used to constrain systematics and backgrounds, oscillations should also be considered for these samples.

Figure 4 presents our results in a consistent four-neutrino approach, considering oscillations of all ν_e and ν_μ samples. We show the MicroBooNE-Inclusive 95% C.L. constraints on Δm^2_{41} and $\sin^2(2\theta_{ee}) \equiv 4|U_{e4}|^2(1-|U_{e4}|)^2$ (top panel) or $\sin^2(2\theta_{\mu\mu}) \equiv 4|U_{\mu 4}|^2(1-|U_{\mu 4}|)^2$ (bottom panel). In each panel of Fig. 4 we perform two analyses (both in blue): solid lines present the constraint on a mixing angle when the other is fixed to zero, whereas dashed lines present the constraint when we profile over the other

mixing angle. The disappearance prospects for ν_e are compared against hints of sterile neutrinos in gallium experiments [49–53] and constraints from solar [54], and reactor antineutrino [55–61] experiments. The bottom panel, showing MicroBooNE ν_μ disappearance constraints, is contrasted against constraints from MINOS/MINOS+ [62] and results from IceCube [63], including a 90% C.L. preferred region and a best-fit point. For further justification of this test-statistic and coverage studies for both Figs. 3 and 4, see the Supplemental Material [27].

As we see, even in the absence of neutrino appearance, i.e., U_{e4} or $U_{\mu 4}$ equal zero, MicroBooNE can still set a limit on neutrino disappearance. For muon neutrinos, the disappearance sensitivity comes from the large ν_μ data sample. For electron neutrinos, in turn, the sensitivity derives from the large ν_e background.

As one final remark on the importance of the complete four-neutrino analysis, Fig. 5 shows the 3σ C.L. constraint from MicroBooNE-Inclusive as a function of $\sin^2(2\theta_{\mu e})$ after profiling over $\sin^2(2\theta_{\mu\mu})$ in comparison with 1σ and 3σ CL preferred regions of MiniBooNE under the same set of assumptions [64]. Even more than in Fig. 3, we see that 3σ-C.L.-allowed MiniBooNE parameter space persists despite the MicroBooNE-inclusive constraints.

Our results emphasize that, while the signal-oscillation-only analysis is simple and intuitive, accounting for oscillations in *all* samples is the only fully consistent approach and can affect the interpretation of the results. This will be even more relevant for the full SBN program, particularly due to different oscillation effects among the three detectors as well as due to the increased analysis sensitivity. We *strongly* advocate for the adoption of this standard moving forward with short-baseline searches for anomalous neutrino (dis)appearance.

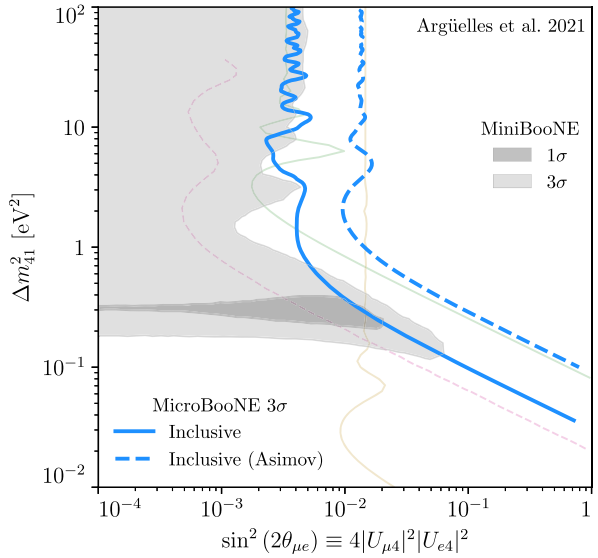

FIG. 5. MicroBooNE constraint on Δm^2_{41} and $\sin^2(2\theta_{\mu e})$ after profiling over the unshown mixing angle in a consistent four-neutrino analysis. Preferred MiniBooNE regions [64] are shown in gray. Other constraints or projections, faded for clarity, are identical to those in Fig. 3.

In this complete picture, we find results consistent with no oscillations, with a best-fit point at $\Delta m^2_{41} = 1.38$ eV^2, $\sin^2(2\theta_{ee}) = 0.2$, and $\sin^2(2\theta_{\mu\mu}) = 0$ with a significance of 0.4σ. Our results do not agree with Ref. [65]. We believe that this stems from the treatment of systematic uncertainties, as we consider correlated systematics by using [29]; and due to the fact that we account for oscillations in the partially contained ν_e sample, which is used to obtain the constrained fully contained ν_e sample. We also implement oscillations as a function of true neutrino energy.

Conclusions.—Does MicroBooNE rule out the ν_e interpretation of the MiniBooNE low-energy excess? And does it disfavor the sterile neutrino explanation of the excess? While current MicroBooNE analyses give us invaluable insights on the MiniBooNE anomaly, we find that they still do not provide definitive answers to either of these two questions. Uncertainties on MiniBooNE backgrounds significantly impact MicroBooNE's reach, and consequently, the MiniBooNE puzzle remains wide open. To demonstrate this quantitatively, we have developed a model-independent analysis and we have carried out a fully consistent sterile neutrino fit of MicroBooNE data in the context of the MiniBooNE excess. In the first analysis, we find MiniBooNE excess spectra with goodness-of-fit better than 10% that are allowed by MicroBooNE data at $< 2\sigma$. In the sterile neutrino analysis, we find that MicroBooNE's 3σ exclusion does not cover the entire MiniBooNE LEE allowed region.

Our findings highlight the importance of running the full SBN program, and of complementing it with the worldwide efforts to search for light sterile neutrinos in reactor [66–70], radioactive source [49], accelerator [71–74], solar [54,75], and atmospheric neutrino [63,76–80] experiments. Together, these experiments will have sufficient sensitivity to answer this decades-old puzzle once and for all.

We are particularly grateful to John Beacom and Steven Prohira for invaluable discussions and involvement in the early stages of this work. We thank Jeff Berryman and Bryce Littlejohn for discussions regarding reactor antineutrino measurements. P. M. is grateful to several members of CCAPP at Ohio State University for many discussions on the MicroBooNE results. Fermilab is operated by the Fermi Research Alliance, LLC under Contract No. DE-AC02-07CH11359 with the United States Department of Energy. This project has received support from the European Union's Horizon 2020 research and innovation program under the Marie Skłodowska-Curie grant agreement No. 860881-HIDDeN. C. A. A. is supported by the Faculty of Arts and Sciences of Harvard University, and the Alfred P. Sloan Foundation. I. M. S. is supported by the Faculty of Arts and Sciences of Harvard University. Perimeter Institute is supported by the Government of

Canada through the Department of Innovation, Science and Economic Development and by the Province of Ontario through the Ministry of Research, Innovation and Science.

[1] K. N. Abazajian *et al.*, arXiv:1204.5379.
[2] A. Aguilar *et al.* (LSND Collaboration), Phys. Rev. D **64**, 112007 (2001).
[3] A. A. Aguilar-Arevalo *et al.* (MiniBooNE Collaboration), Phys. Rev. D **103**, 052002 (2021).
[4] B. Dasgupta and J. Kopp, Phys. Rep. **928**, 1 (2021).
[5] C. A. Argüelles, K. Farrag, T. Katori, R. Khandelwal, S. Mandalia, and J. Salvado, J. Cosmol. Astropart. Phys. 02 (2020) 015.
[6] D. F. G. Fiorillo, G. Miele, S. Morisi, and N. Saviano, Phys. Rev. D **101**, 083024 (2020).
[7] D. Fiorillo, G. Miele, S. Morisi, and N. Saviano, Phys. Rev. D **102**, 083014 (2020).
[8] P. Abratenko *et al.* (MicroBooNE Collaboration), Phys. Rev. Lett. **128**, 111801 (2022).
[9] P. Abratenko *et al.* (MicroBooNE Collaboration), arXiv:2110.14054.
[10] P. Abratenko *et al.* (MicroBooNE Collaboration), companion paper, Phys. Rev. D Phys. Rev. D **105**, 112005 (2022).
[11] P. Abratenko *et al.* (MicroBooNE Collaboration), companion paper, Phys. Rev. D **105**, 112003 (2022).
[12] P. Abratenko *et al.* (MicroBooNE Collaboration), companion paper, Phys. Rev. D **105**, 112004 (2022).
[13] S. Palomares-Ruiz, S. Pascoli, and T. Schwetz, J. High Energy Phys. 09 (2005) 048.
[14] Y. Bai, R. Lu, S. Lu, J. Salvado, and B. A. Stefanek, Phys. Rev. D **93**, 073004 (2016).
[15] Z. Moss, M. H. Moulai, C. A. Argüelles, and J. M. Conrad, Phys. Rev. D **97**, 055017 (2018).
[16] M. Dentler, I. Esteban, J. Kopp, and P. Machado, Phys. Rev. D **101**, 115013 (2020).
[17] A. de Gouvêa, O. L. G. Peres, S. Prakash, and G. V. Stenico, J. High Energy Phys. 07 (2020) 141.
[18] M. Hostert and M. Pospelov, Phys. Rev. D **104**, 055031 (2021).
[19] B. Armbruster *et al.* (KARMEN Collaboration), Phys. Rev. D **65**, 112001 (2002).
[20] N. Agafonova *et al.* (OPERA Collaboration), J. High Energy Phys. 07 (2013) 004; 07 (2013) 085(A).
[21] M. Antonello *et al.* (ICARUS Collaboration), Eur. Phys. J. C **73**, 2599 (2013).
[22] P. Astier *et al.* (NOMAD Collaboration), Phys. Lett. B **570**, 19 (2003).
[23] L. Borodovsky *et al.*, Phys. Rev. Lett. **68**, 274 (1992).
[24] GitHub repository: https://github.com/Harvard-Neutrino/MicroBooNE-analysis-2021 (2021).
[25] To directly compare with MicroBooNE results, we base our analysis on the 2018 MiniBooNE data [26].
[26] A. A. Aguilar-Arevalo *et al.* (MiniBooNE Collaboration), Phys. Rev. Lett. **121**, 221801 (2018).
[27] See Supplemental Material at http://link.aps.org/supplemental/10.1103/PhysRevLett.128.241802 for additional details on our statistical analysis.
[28] We note that the two samples are not statistically independent, as certain events will be present in both datasets. Therefore, the constraints that we derive from the two samples should be viewed as separate and should not combined as if they were independent.
[29] P. Abratenko *et al.* (MicroBooNE Collaboration), MicroBooNE 1*eX* Data Release (2021).
[30] P. Abratenko *et al.* (MicroBooNE Collaboration), MicroBooNE CCQE Data Release (2021).
[31] X. Ji, W. Gu, X. Qian, H. Wei, and C. Zhang, Nucl. Instrum. Methods Phys. Res., Sect. A **961**, 163677 (2020).
[32] D. Foreman-Mackey, D. W. Hogg, D. Lang, and J. Goodman, Publ. Astron. Soc. Pac. **125**, 306 (2013).
[33] We would like to stress that our goal is *not* to reassess the MiniBooNE backgrounds, but to use them as a proxy to generate MBLEE shapes. Alternatively, we have also generated templates by independently varying the excess events in each bin. Both approaches produce very similar results.
[34] A. A. Aguilar-Arevalo *et al.* (MiniBooNE Collaboration), arXiv:2110.15055.
[35] G. D'Agostini, Nucl. Instrum. Methods Phys. Res., Sect. A **362**, 487 (1995).
[36] M. Collaboration, MicroBooNE low-energy excess signal prediction from unfolding MiniBooNE Monte-Carlo and data, Report No. MICROBOONE-NOTE-1043-PUB, 2018.
[37] A. Aguilar-Arevalo *et al.* (PIENU Collaboration), Phys. Lett. B **798**, 134980 (2019).
[38] M. Collaboration, Instructions on how to use Dec 2010 MiniBooNE public data for muon-to-electron antineutrino oscillation fits (2010).
[39] S. S. Wilks, Ann. Math. Stat. **9**, 60 (1938).
[40] S. Algeri, J. Aalbers, K. Dundas Morå, and J. Conrad, Nat. Rev. Phys. **2**, 245 (2020).
[41] S. Gariazzo, C. Giunti, M. Laveder, Y. F. Li, and E. M. Zavanin, J. Phys. G **43**, 033001 (2016).
[42] A. Diaz, C. A. Argüelles, G. H. Collin, J. M. Conrad, and M. H. Shaevitz, Phys. Rep. **884**, 1 (2020).
[43] S. Böser, C. Buck, C. Giunti, J. Lesgourgues, L. Ludhova, S. Mertens, A. Schukraft, and M. Wurm, Prog. Part. Nucl. Phys. **111**, 103736 (2020).
[44] M. Dentler, A. Hernández-Cabezudo, J. Kopp, P. A. N. Machado, M. Maltoni, I. Martinez-Soler, and T. Schwetz, J. High Energy Phys. 08 (2018) 010.
[45] More concretely, we use the data releases provided along with Refs. [10,29] to determine the expected $\nu_{\mu,e}$ CC fully and partially contained spectra as a function of *true* neutrino energy. Oscillations are included with respect to true energy, then the distributions are mapped into *reconstructed* neutrino energy (again, using Ref. [29]) where test statistics are calculated.
[46] P. A. Machado, O. Palamara, and D. W. Schmitz, Annu. Rev. Nucl. Part. Sci. **69**, 363 (2019).
[47] N. Agafonova *et al.* (OPERA Collaboration), J. High Energy Phys. 06 (2018) 151.
[48] J. Kopp, P. A. N. Machado, M. Maltoni, and T. Schwetz, J. High Energy Phys. 05 (2013) 050.
[49] V. V. Barinov *et al.*, arXiv:2109.11482 [Phys. Rev. Lett. (to be published)].
[50] J. N. Abdurashitov *et al.* (SAGE Collaboration), Phys. Rev. C **59**, 2246 (1999).

[51] J. N. Abdurashitov *et al.*, Phys. Rev. C **73**, 045805 (2006).
[52] M. Altmann *et al.* (GNO Collaboration), Phys. Lett. B **616**, 174 (2005).
[53] F. Kaether, W. Hampel, G. Heusser, J. Kiko, and T. Kirsten, Phys. Lett. B **685**, 47 (2010).
[54] K. Goldhagen, M. Maltoni, S. Reichard, and T. Schwetz, Eur. Phys. J. C **82**, 116 (2022).
[55] J. M. Berryman and P. Huber, J. High Energy Phys. 01 (2021) 167.
[56] Y. Declais *et al.*, Nucl. Phys. **B434**, 503 (1995).
[57] I. Alekseev *et al.* (DANSS Collaboration), Phys. Lett. B **787**, 56 (2018).
[58] D. Adey *et al.* (Daya Bay Collaboration), Phys. Rev. Lett. **121**, 241805 (2018).
[59] H. de Kerret *et al.* (Double Chooz Collaboration), Nat. Phys. **16**, 558 (2020).
[60] Y. J. Ko *et al.* (NEOS Collaboration), Phys. Rev. Lett. **118**, 121802 (2017).
[61] G. Bak *et al.* (RENO Collaboration), Phys. Rev. Lett. **121**, 201801 (2018).
[62] P. Adamson *et al.* (MINOS+ Collaboration), Phys. Rev. Lett. **122**, 091803 (2019).
[63] M. G. Aartsen *et al.* (IceCube Collaboration), Phys. Rev. Lett. **125**, 141801 (2020).
[64] V. Brdar and J. Kopp, arXiv:2109.08157.
[65] P. B. Denton, arXiv:2111.05793.
[66] N. Allemandou *et al.* (STEREO Collaboration), J. Instrum. **13**, P07009 (2018).
[67] J. Ashenfelter *et al.* (PROSPECT Collaboration), Nucl. Instrum. Methods Phys. Res., Sect. A **922**, 287 (2019).
[68] I. Alekseev *et al.*, J. Instrum. **11**, P11011 (2016).
[69] A. P. Serebrov *et al.*, Phys. Rev. D **104**, 032003 (2021).
[70] M. Licciardi (Stereo Collaboration), in *Proceedings of the 55th Rencontres de Moriond on Electroweak Interactions and Unified Theories* (2021), arXiv:2105.13776.
[71] S. Ajimura *et al.*, arXiv:1705.08629.
[72] F. Suekane (JSNS2 Collaboration), Proc. Sci., NuFact2019 (**2020**) 129.
[73] J. Alonso, C. A. Argüelles, J. M. Conrad, Y. D. Kim, D. Mishins, S. H. Seo, M. Shaevitz, J. Spitz, and D. Winklehner, Phys. Rev. D **105**, 052009 (2022).
[74] J. R. Alonso *et al.*, arXiv:2110.10635.
[75] A. de Gouvêa, E. McGinness, I. Martinez-Soler, and Y. F. Perez-Gonzalez, arXiv:2111.02421.
[76] K. Abe *et al.* (Super-Kamiokande Collaboration), Phys. Rev. D **91**, 052019 (2015).
[77] A. Albert *et al.* (ANTARES Collaboration), J. High Energy Phys. 06 (2019) 113.
[78] B. R. Smithers, B. J. P. Jones, C. A. Argüelles, J. M. Conrad, and A. Diaz, Phys. Rev. D **105**, 052001 (2022).
[79] A. Domi and J. Coelho (KM3NeT, ANTARES Collaborations), Proc. Sci., ICRC2019 (**2021**) 870.
[80] Y. Wang and O. Yasuda, Prog. Theor. Exp. Phys. **2022**, 023B04 (2022).